Received: 5 November 2018 | Revised: 8 March 2019 | Accepted: 4 April 2019

DOI: 10.1002/bip.23283

FULL PAPER

Biopolymers WILEY

Peptoid microsphere coatings: The effects of helicity, temperature, pH, and ionic strength

German R. Perez Bakovic | Jesse L. Roberts | Bryce Colford | Myles Joyce | Shannon L. Servoss

Ralph E. Martin Department of Chemical Engineering, University of Arkansas Fayetteville, Fayetteville, Arkansas

Correspondence
Shannon L. Servoss, Ralph E. Martin Department of Chemical Engineering, University of Arkansas Fayetteville, Fayetteville, Arkansas.
Email: sservoss@uark.edu

Funding information
Arkansas Biosciences Institute; Arkansas EPSCoR Program, ASSET III; Center for Advanced Surface Engineering, Grant/Award Number: IIA-1457888

Abstract

Peptoids are peptidomimetic oligomers that predominantly harness similarities to peptides for biomimetic functionality. They have potential for use in biomedical applications and biosensors due to resistance to proteolytic degradation and low immunogenicity. The incorporation of chiral, aromatic side chains in the peptoid sequence allows for the formation of distinct secondary structures and self-assembly into supramolecular assemblies, including microspheres. Peptoid microspheres can be coated onto substrates for potential use in biosensor technologies, tissue engineering platforms, and drug-delivery systems. In order to be useful for these applications, the peptoid coatings must be robust under physiological conditions. In this study, we report the effects of various conditions on the peptoid microsphere coatings, including (i) helicity, (ii) temperature, (iii) pH, and (iv) ionic strength. These studies show that microsphere size decreases with increasing peptoid helicity and the positively charged side chains are positioned on the outside of the microspheres. The peptoid microsphere coatings are robust under physiological conditions but degrade in acidic conditions (pH < 7) and at low ionic strengths (<150 μM).

KEYWORDS
biopolymer, coatings, microspheres, peptoid

1 | INTRODUCTION

Natural polymers, such as proteins and peptides, have inspired the development of synthetic materials that mimic the fundamental molecular features, and are therefore also able to mimic the function.[1] While proteins and peptides have a myriad of unique functional properties, as biomaterials they are limited due to proteolytic degradation and as a result are restricted in their potential for use in biomedical and therapeutic applications.[2] Efforts to overcome these limitations have led to the design and development of innovative peptidomimetic oligomers.[3–8] These synthetic oligomer analogs largely exploit structural similarities to allow for bioactive functionalities. Some bioactive roles are determined by the unique ability of proteins and peptides to self-assemble into complex, sequence-specific secondary and supramolecular structures.[9] Specific peptidomimetic oligomers, commonly referred to as foldamers,[10] display well-defined secondary structures, and are therefore of great interest for use in biomaterials.

One class of foldamers, peptoids or poly-N-substituted glycines, closely resemble peptides, with the side chains attached to the backbone amide nitrogen rather than the backbone α-carbon as in peptides. This seemingly minor modification to the backbone has important implications to peptoid structure and function, including reduced proteolytic degradation that makes them a promising alternative to peptides for therapeutic applications where proteolysis is of major concern. The backbone modification also prevents hydrogen bonding within the backbone, which is critical for the formation of secondary structure in peptides. However, including specific side chains can induce the formation of peptoid secondary structures such as turns,[11,12] loops,[13] and

helices[14–18] that allow for the formation of supramolecular assemblies.[19–24] For peptoid homooligomers of (S)-methylbenzylamine, stable helices are formed with as few as five monomer units and full helicity is reached at 13 monomer units.[9] The circular dichroism (CD) spectra strongly resembles that for protein α-helices[9] and NMR confirms a helical structure similar to protein polyproline type-I helices, with a periodicity of three residues per turn and a helical pitch of ~6 Å.[16] Like peptides, peptoids are constructed via solid-phase synthesis, but following a submonomer method that provides a robust and highly efficient synthesis platform with precise sequence control.[25] Side chains are introduced by the incorporation of commercially available primary amines, enabling access to more than 300 side chain chemistries.[1]

Previous work has focused on the effects of peptoid water solubility, helical content, charge placement, and side chain bulk on self-assembly into microspheres.[24] Both peptoid helicity and partial water solubility were found to be crucial for microsphere formation. The microspheres (0.3-3.6 μM) are orders of magnitude larger than the length of a single peptoid helix (∼24 Å), suggesting that larger peptoid groupings are formed by stacking of the chiral aromatic groups.[24] Aromatic stacking has been observed in similar types of supramolecular assemblies for both peptides and peptoids.[22,26–29] Further, peptoid sequences with alternating positive and negative charges on one face of the helix produce smaller microspheres (~0.3 μM) as compared to those with alternating positive and neutral charges on one face of the helix (~1.5 μM). It is believed that the opposite charges interact to form tighter helices, resulting in smaller microspheres.[24] Further work in the Servoss lab investigated the factors that affect the reproducible formation of microsphere coatings including solvent effects, administration technique, and drying conditions.[30] These studies showed that reproducible coatings were formed by solubilizing the peptoid in an aqueous solution of protic solvent, completely covering the surface with solution, and allowing it to dry at room temperature with 60% humidity.

Potential applications for peptoid microspheres include biosensors, artificial extracellular matrices, and drug delivery systems. The customizability of the microsphere chemistry allows for the fine-tuning based on application or environment. The work reported here shows the effect of peptoid length (and in turn helicity) on microsphere size, as well as the effects of temperature, pH, and ionic strength on the robustness of peptoid microsphere coatings. The surface charge and phase transition temperatures of the different peptoid lengths were measured using zeta potential and differential scanning calorimetry (DSC), respectively. Scanning electron microscopy (SEM) and ImageJ processing show that as peptoid chain length, or helicity, is increased microsphere size decreases and the size distribution increases. Zeta potential proved that there is a positive charge located on the outer surface of the peptoid microspheres, and DSC showed that the melting temperatures ranged from 78 to 83 °C for the various peptoid lengths. Furthermore, SEM confirmed that the microsphere coatings are extremely robust under physiological conditions; however, they degraded in low ionic strength and low pH solutions.

2 | MATERIALS AND METHODS

2.1 | Materials

(S)-methylbenzylamine and 4-methoxybenzylamine were purchased from Acros Organics (Pittsburgh, PA). *tert*-butyl N-(4-aminobutyl)carbamate was purchased from CNH Technologies Inc. (Woburn, MA). MBHA rink amide resin was purchased from NovaBiochem (Gibbstown, NJ). Piperidine was purchased from Sigma-Aldrich (St. Louis, MO). Ultra clean glass microarray slides, and disuccinimidyl suberate (DSS) were purchased from Thermo Scientific (Pittsburgh, PA). All other reagents were purchased from VWR (Radnor, PA). All chemicals were used without further modifications unless otherwise specified.

2.2 | Peptoid synthesis, purification, and characterization

Peptoids were synthesized following a submonomer, solid-phase method on rink amide resin, as previously described.[25,31] Synthesis follows a carboxy to amino direction and the submonomer method includes two steps: acylation to extend the backbone and nucleophilic substitution to incorporate the side chain.[32] Briefly, the resin was swelled with dimethylformamide (DMF), and the Fmoc protecting group was removed using a 20% solution of piperidine in DMF. The resin-bound secondary amine was acylated with 0.4 M bromoacetic acid in DMF in the presence of N,N′-diisopropyl carbodiimide, mixing for 1 minute. Amine submonomers were incorporated via an S_N2 nucleophilic substitution reaction with 0.5 M primary amine in DMF, mixing for 2 minutes. The two-step acylation and nucleophilic substitution cycle was repeated until the desired sequence was obtained. The peptoid was cleaved from the resin using a mixture of 95% trifluoroacetic acid (TFA), 2.5% water, and 2.5% triisopropylsilane.

Peptoids were purified using a Waters Delta 600 preparative high-performance liquid chromatography (HPLC) instrument (Milford, MA) with a Duragel G C18 150 × 20 mm column (Peeke Scientific, Novato, CA) and a linear gradient of 35% to 95% solvent B (acetonitrile, 5% water, 0.1% TFA) in A (water, 5% acetonitrile, 0.1% TFA), over 60 minutes. Peptoids were confirmed to be >98% pure via analytical HPLC (Waters Alliance) with a Duragel G C18 150 × 2.1 mm column (Peeke Scientific) using a linear gradient of 35% to 95% solvent D (acetonitrile, 0.1% TFA) in C (water, 0.1% TFA), over 30 minutes. Presence of the desired sequence was confirmed via matrix assisted laser desorption/ionization time of flight (MALDI-TOF) mass spectrometry (Bruker, Billerica, MA). Purified peptoid fractions were lyophilized and stored as a powder at −20 °C.

2.3 | Circular dichroism

Peptoid secondary structure was confirmed via circular dichroism (CD) spectroscopy using a Jasco J-715 instrument (Easton, MD). The peptoids were dissolved in methanol at a concentration of 60 μM. Data was collected at room temperature with a scanning speed of

20 nm/min in a cuvette with a path length of 0.2 mm. Each spectrum was the average of 20 accumulations.

2.4 | Peptoid microsphere coatings

Peptoid microspheres were prepared by dissolving the peptoid in a 4:1 ethanol/water (v/v) solution at a concentration of 5 mg/mL. The peptoid solution was applied to glass substrates using a pipette and allowed to dry at room temperature and 60% relative humidity for 1 hour. Coating morphology was imaged using a Phillips XL-30 environmental scanning electron microscope (SEM; FEI, Hillsboro, OR).

2.5 | Microsphere size analysis

Particle size analysis was performed using ImageJ software (National Institute of Health, MD). Noise reduction was completed with a fast Fourier transform (FFT) band-pass filter normalization, eliminating low- and high-spatial frequencies and transforming the original SEM images to a two-dimensional representation of the frequency. The images were converted to 8-bit grayscale and binarized adjusting the white and black threshold to optimize particle contrast with the background. Greater than 200 particles were manually evaluated for each experimental condition and plotted using Origin2018.

2.6 | Surface charge measurements

The surface charge of the peptoid microspheres was measured in terms of zeta potential using a Beckman Coulter Delsa NanoHC instrument (Brea, CA). A flat cell was employed for determination of the zeta potential of the peptoid microspheres. The peptoid microsphere coatings were submerged in the feed solution that was set at a neutral pH of 7.0 and the measurements were taken.

2.7 | Differential scanning calorimetry

The melting temperature and phase transition properties of the peptoid microspheres were measured using a TA Instruments Differential Scanning Calorimeter Model 25 (New Castle, DE). The peptoid microspheres were formed by dissolving peptoid in a 4:1 ethanol/water (v/v) solution at a concentration of 3 mg/mL. The peptoid microspheres were deposited onto a TA Instruments Tzero aluminum pan at a constant volume of 60 μL. The pan was set in a holding vessel where a lid was hermetically sealed using a specialized Tzero Press. Individual sample masses were taken and documented in the DSC control software TRIOS v4.4, where, after temperature equilibration at 0 °C, an isothermal period of 10 minutes was completed. The ramping period of 20 °C per minute up to a maximum temperature of 200-240 °C was used to determine the phase transition and melting temperature of the peptoid microspheres. Upon conclusion, the plot of normalized heat flow (W/g) vs temperature (°C) was analyzed and the peak integration function within TRIOS resulted in the normalized enthalpy (J/g) and peak temperature (°C) for phase change.

2.8 | Coating robustness under biological assay conditions

The robustness of the peptoid microsphere coatings was assessed by incubation in solutions common to bioanalytical assays that have various values of pH and ionic strengths. Specifically, the coatings were incubated in 10 mg/mL casein in phosphate-buffered saline (PBS; pH 7.3, ionic strength 150 mM) for 1 hour, 0.05% Tween in PBS (PBS-T; pH 7.3, ionic strength 150 mM) for 12 hours, 0.003% hydrogen peroxide in 0.1 M sodium borate (pH 8.2, ionic strength 600 mM) for 10 minutes, and nanopure water (pH ~7, ionic strength ~0 mM) for up to 30 minutes.

2.9 | Effect of temperature, pH, and ionic strength on coating

The ability of the peptoid microsphere coatings to withstand temperature, pH, and ionic strength was assessed through incubation in various solutions. The effect of temperature was evaluated by incubating the peptoid microsphere coatings in PBS and water at 37 °C. The temperature of both PBS and nanopure water was preheated and kept constant at 37 °C using a covered incubation chamber and hot plate. The pH and ionic strength robustness studies were assessed by incubating the peptoid microsphere coatings in solutions ranging from pH 3 to 11 and ionic strength of 0 to 500 mM at room temperature (25 °C). The solution pH was adjusted by adding a stock hydrochloric acid or sodium hydroxide solution drop-wise until the desired pH was attained. The coatings were incubated in solutions of different pH values (pH = 3, 4, 5, 6, 7, 8, 9, 10, 11) for 1 hour. The ionic strength of water and PBS was adjusted using a stock potassium chloride solution until the desired ionic strengths were obtained. The coatings were incubated in solutions of different ionic strength values (ionic strength = 0, 50, 100, 150, 250, 500 mM) for 1 hour. The robustness of the peptoid microsphere coatings was assessed via SEM by analyzing microsphere morphology and surface coverage.

3 | RESULTS

3.1 | Peptoid sequence and characterization

The peptoid sequences used in this study (Figure 1A) are based on that of a helical and partially water soluble 12mer that was previously reported to form microspheres.[24] Helical secondary structure is induced by including two-thirds chiral, aromatic side chains (Nspe) such that two faces of the helix contain Nspe side chains (Figure 1B). This configuration allows for interactions between the benzene rings on different peptoid molecules. The third face of the peptoid helix contains alternating side chains with amine and methoxybenzyl groups to increase water solubility, as well as facilitate attachment to glass substrates. In this study, the length of the peptoid was varied by repeating the same six monomer unit for final lengths of 6, 12, 18, and 24 monomers (Figure 1A).

Peptoid helicity was assessed by CD spectroscopy (Figure 2). The 12mer, 18mer, and 24mer peptoids exhibit a maximum near 193 nm and two minima near 208 and 222 nm, indicative of polyproline

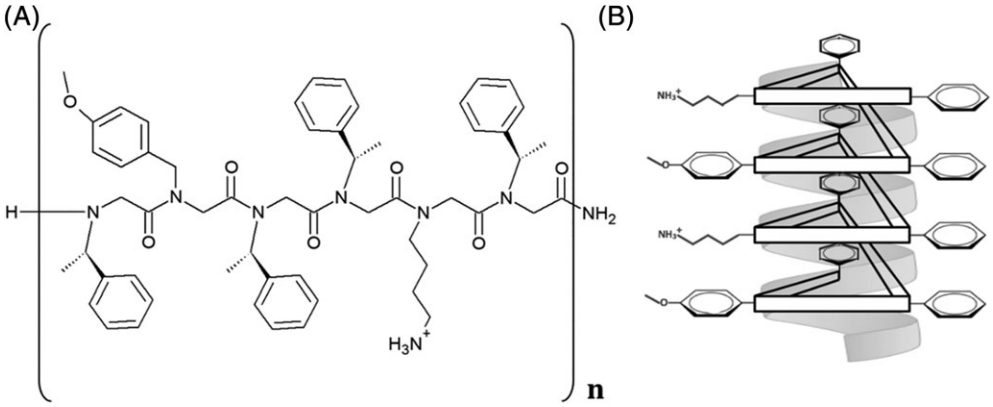

FIGURE 1 A, Linear peptoid sequence. Four peptoids were studied: 6mer (n = 1, MW = 968), 12mer (n = 2, MW = 1919), 18mer (n = 3, MW = 2870), and 24mer (n = 4, MW = 3821). B, Representation of the 12mer peptoid helix

type-I-like peptoid helices.[32] The 6mer also displayed a maximum near 193 nm and a minima near 222 nm; however, a second minima at 200 nm indicates both random coil and polyproline type-I-like peptoid helix secondary structures.[33] The relative helicity increases with peptoid length, as evidenced by the increasing intensity of the minimum peak at 222 nm.[34] This corresponds to previous studies which have shown that peptoid helicity increases with peptoid length.[9] This is further corroborated by molecular simulations.[35] These studies, which were validated by NMR experiments, show that peptoid helix formation is a function of temperature and chain length ultimately proving that as chain length increases helicity increases and peptoid helix formation is thermodynamically favorable.[35,36]

3.2 | Effect of helicity on microsphere size and distribution

It is desirable to tune the size of microspheres for different applications. Based on our previous results,[30] we hypothesized that peptoids with tighter helicity would form smaller microspheres. The formation of microspheres by peptoids with different helicities (6mer, 12mer, 18mer, and 24mer) was tested. The peptoids were solubilized in 4:1 ethanol:

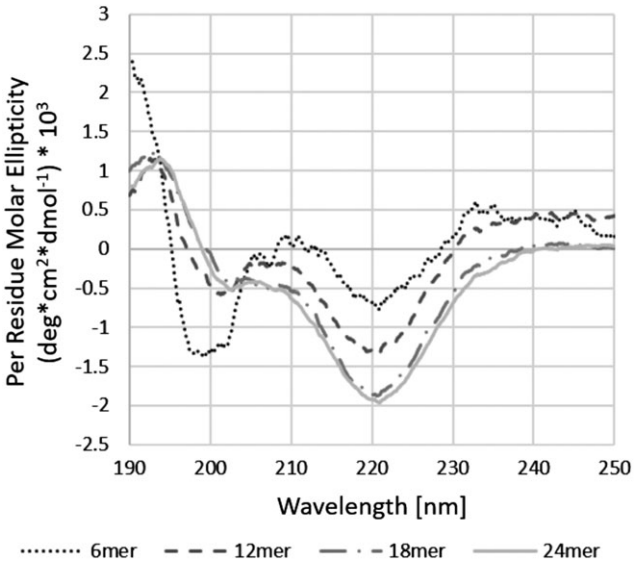

FIGURE 2 Circular dichroism spectra for 6mer, 12mer, 18mer, and 24mer peptoid in methanol at 60 μM

water and dried on glass substrates to form the microsphere coatings. Microsphere size was visually assessed by SEM and measured using ImageJ software. The 6mer peptoid did not form microspheres (Figure S1 in Supplemental Information), likely due to decreased helicity, increased water solubility, and the limited number of aromatic side chains to induce stacking. The 12mer, 18mer, and 24mer peptoids all formed microspheres of different sizes (Figure 3A-C, respectively). As expected, microsphere diameter decreased with increasing helicity, with average diameters of 2.26 μM, 1.91 μM, and 1.24 μM for the 12mer, 18mer, and 24mer peptoids, respectively.

The decrease in size is likely due to the increased interactions between the peptoids that have higher helical content, and therefore closer packing in the microspheres. Conversely, peptoids with looser helical structure are not able to pack as tightly and form larger microspheres. In addition, there is a direct relationship between peptoid length and microsphere size distribution, with the most uniform size distribution observed for the 12mer peptoid (Figure 3A,D) and the most disperse sizes observed for the 24mer peptoid (Figure 3C,F).

Like the peptoid microspheres, peptide foldamers use their molecular interactions to form distinct secondary structures that can be tailored into self-assembling supramolecular structures (spherical micelles,[37] worm-like micelles,[38] lamellar sheets,[39] vesicles,[40] nanotubes,[41] and fibrils[42]). The size of spherical micelles formed from thermally responsive elastin-like peptides can be tuned through the secondary structure by altering the total chain length and the hydrophilic-hydrophobic chain ratio in the peptide.[37] Peptide nanotubes can be formed by incorporated cyclic peptides with D- and L-amino acids that self-assemble through antiparallel hydrogen bonding and stereochemical interactions of the peptide backbone.[43] By strategically assembling the peptide entities at specific ratios and altering the number of amino acids, the overall length and size of the peptide nanotube can be controlled for desirable end-product formation.[44] These supramolecular structures prove that the overall size is a function of secondary structure and intermolecular interactions, like the helicity of the peptoid microspheres.

3.3 | Surface charge of peptoid microspheres

The surface charge, or zeta potential, of the different length peptoids was obtained using electrophoretic light scattering (ELS). The zeta potential gives the potential difference between the solid-liquid

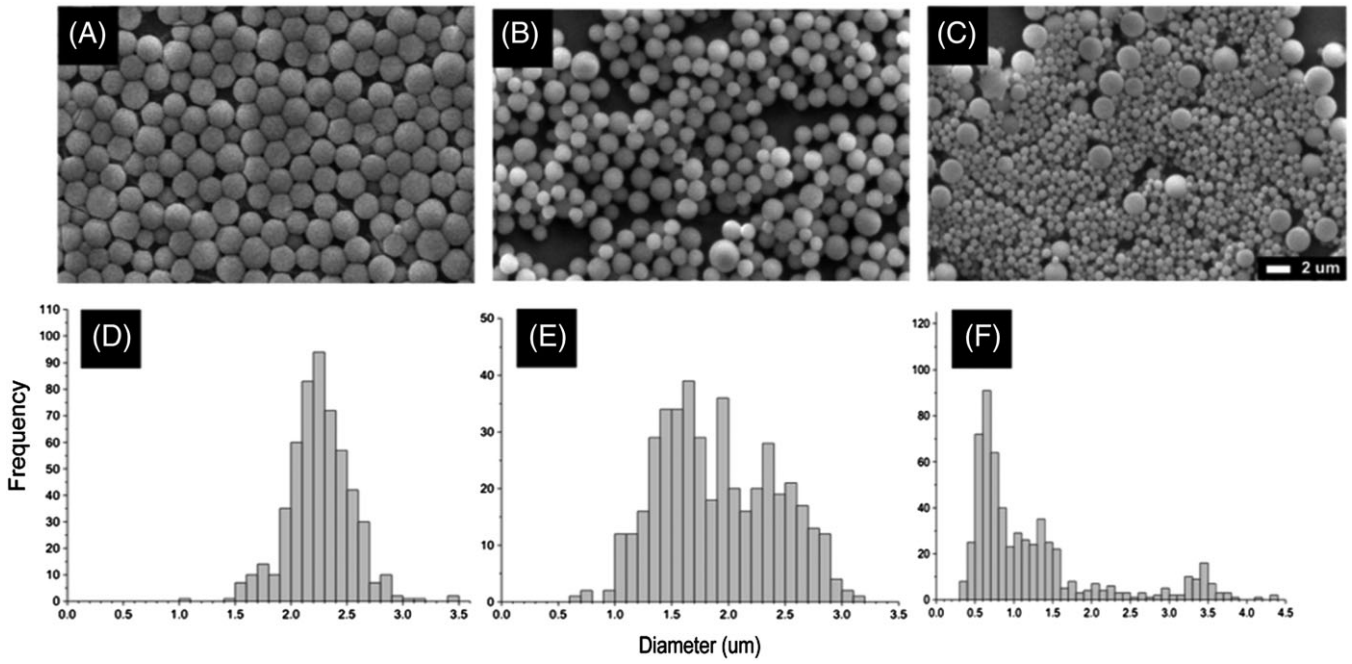

FIGURE 3 SEM images of (A) 12mer, (B) 18mer, and (C) 24mer peptoid microspheres. The size distribution for (D) 12mer, (E) 18mer, and (F) 24mer was evaluated using ImageJ software

interface of the charged particle and the liquid media. It is hypothesized that the positively charged side chains are located on the outside of the microspheres due to the stacking of the aromatic groups, as well as the ability of the peptoid microspheres to robustly attach to glass surfaces that have a relative negative charge. The surface zeta potential of the peptoid microspheres showed a drastic increase as compared to the ultraclean glass (Figure 4). The difference between the unmodified surface and peptoid-coated substrate indicates that the surface of the peptoid microspheres is positively charged. Although aqueous feed at neutral pH was used (~7.0), the amine side chain can be protonated ($—NH_3^+$) resulting in a net positive charge.[45] An increase in zeta potential as the peptoid chain length increases (12mer = +11.85, 18mer = +28.79, 24mer = +41.64) is potentially due to an increase in the number of cationic side chains, along with the increase in the total number of spheres on the substrate that forms from the tighter helicity.

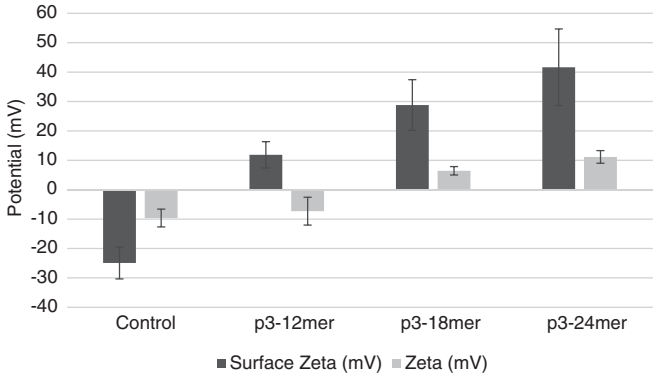

FIGURE 4 Zeta potential measurements for control (4:1 ethanol: water), 12mer, 18mer, and 24mer peptoid microsphere coatings

3.4 | Differential scanning calorimetry measurements

The thermal behavior of the peptoid microspheres was examined by differential scanning calorimetry (DSC) to measure the excess heat capacity as a function of temperature. DSC was run in solid state for the 12mer, 18mer, and 24mer peptoid microspheres to determine the thermodynamic properties of thermally induced phase transitions such as melting temperature (T_m), enthalpy in terms of endothermic vs exothermic peptoid degradation, and the polymorphic nature of the material. As expected, the heat flow was negative for all three peptoid samples, suggesting that the peptoid microsphere degradation occurs endothermically as the peptoid microspheres require heat to break the interactions and bonds during phase transition.[46,47] The phase transition temperature increased as peptoid chain length increased, indicating a correlation between peptoid helicity and thermal stability (Figure 5). The 24mer peptoid microspheres had the highest melting temperature on average at 82.94 ± 0.3845 °C, while the 12mer and 18mer peptoid microspheres were similar at 74.00 ± 4.121 °C and 75.22 ± 4.121 °C, respectively. The broadness in the DSC peaks indicate that the samples are forming polymorphic structures, similar to many common polymers and other microspheres, and at the melting temperature, over 50% of the sample had undergone a phase transition.[48,49]

3.5 | Coating robustness under biological assay conditions

In order to be practical in biomedical applications, the 12mer peptoid microsphere coatings must be robust under various conditions. It was previously observed that the microsphere coatings degrade when exposed to ultrapure water for 24 hours,[30] therefore a thorough

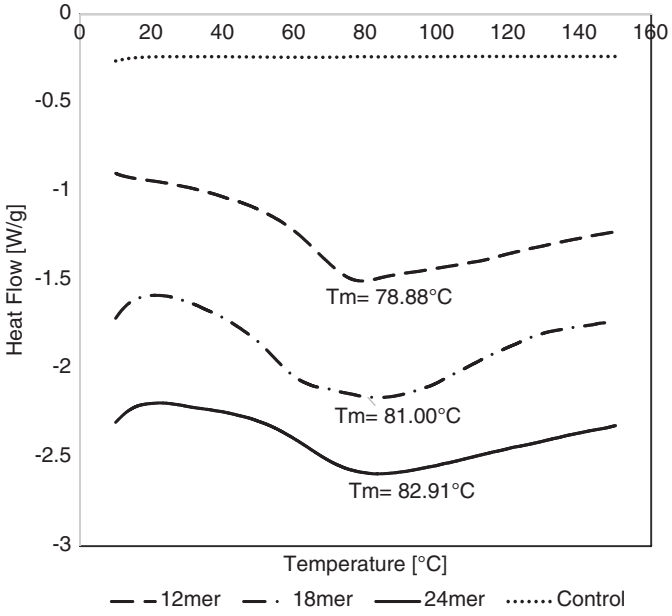

FIGURE 5 Differential scanning calorimetry measurements for control (4:1 ethanol:water), 12mer, 18mer, and 24mer peptoid microsphere coatings

investigation was completed to determine whether pH, ionic concentration, or a combination of the two were responsible. The robustness of 12mer peptoid microsphere coatings was assessed by incubating the coatings in solutions with varying values of pH and ionic strength, including casein in PBS for 1 hour, 0.05% Tween in PBS for 12 hours, 0.003% hydrogen peroxide in 0.1 M sodium borate for 10 minutes, and nanopure water for 10 minutes. The microsphere coatings showed minimum degradation, as assessed by morphology and surface coverage, in all solutions except water (Figure 6A-C and Figure S2 in Supplemental Information). After exposure to water for 30 minutes the microspheres appeared to disintegrate and lift from the surface. Despite the instability of the peptoid microspheres in water, they are robust in PBS for up to 2 months (Figure S3 in Supplemental Information). Based on these preliminary findings, the effects of pH and ionic strength on peptoid microsphere coating robustness has been thoroughly investigated.

3.6 | Effect of temperature on coating robustness

The effect of temperature on the 12mer peptoid microsphere coating robustness was assessed by visually analyzing the coating morphology following incubation in PBS and nanopure water at a physiological temperature of 37 °C for 30 minutes (Figure 7). At this temperature, the peptoid microsphere coatings withstood degradation in all solutions except water. In PBS at 37 °C a small salt layer began forming due to the evaporation and deposition of PBS salts on the glass substrate, but the overall sphere morphology was maintained. After 30 minutes of incubating in water at 37 °C, the microspheres began swelling and lifting from the surface and overall surface coverage was diminished.

3.7 | Effect of pH on coating robustness

The effect of solvent pH on the 12mer peptoid microsphere coating robustness was studied by assessment of coating morphology and coverage following incubation in PBS (Figure 8) with varying pH. Coatings exposed to solutions with pH of 7 or greater are robust, with no significant differences in microsphere morphology or coating coverage (Figure 8A-E). As the solvent starts to approach acidic conditions (pH less than 7), the microsphere morphology and coating coverage deteriorate (Figure 8F-I). These observations are consistent in both PBS and water solutions at similar pH values. These studies were confirmed with water-based solutions (Figure S4 in Supplemental Information). While we do not anticipate changes in pH of the solvent to change the charge state of the peptoids, solubility is increased under acidic conditions.[50] Peptoids with ionizable side chains have been demonstrated to destabilize in response to pH-dependent changes in aqueous solvents.[11,51] In aqueous solvents, the supramolecular structure of the peptoid is ultimately determined by interactions between the side chains and water. In general, polar and charged groups are located on the outside surface due to their stabilization with water, while the hydrophobic residues tend to favor the inside of the structure.[52] The charged and polar residues, specifically lysine in the case of the peptoids studied here, help maintain the solvation necessary to form specific supramolecular structures. Therefore, at higher pH values the pKa of the lysine-like side chain is stabilized by being unprotonated or neutrally charged, maintaining an optimal solvation effect allowing the peptoid microspheres to be robust or less soluble under basic conditions.[53] At low pH (>7) the lysine side chains are below the isoelectric point resulting in a protonated amine group. The protonation forms an energetically less favorable charge solvation structure that results in

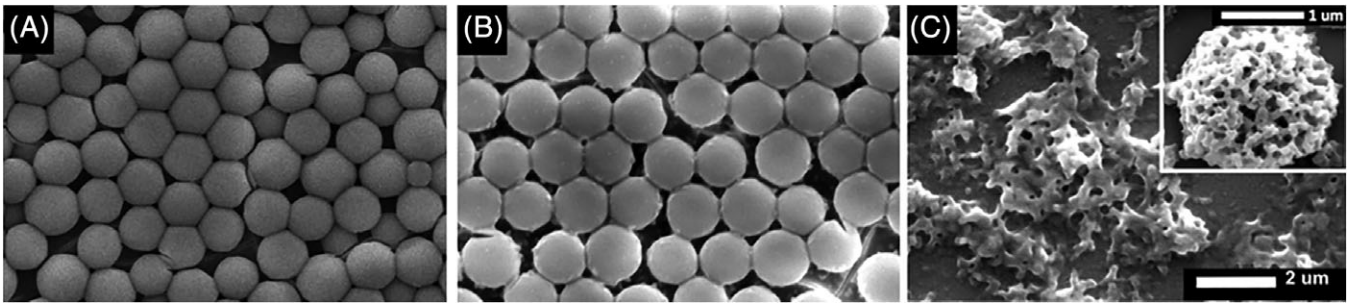

FIGURE 6 SEM images of the peptoid microspheres coatings (A) before incubation, (B) after 24 hour incubation in PBS, and (C) after 30 minute incubation in water with inset showing a high magnification peptoid microsphere

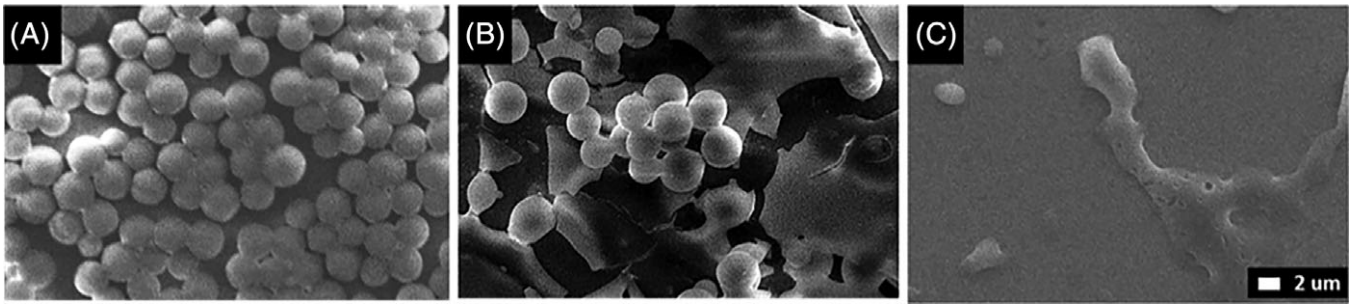

FIGURE 7 SEM images of 12mer peptoid microsphere coatings (A) before incubation, (B) after 30 minute incubation in PBS at 37 °C, and (C) after 30 minute incubation in nanopore water at 37 °C

the destabilization and increased solubility ultimately leading to the deterioration of the peptoid microspheres.[54]

3.8 | Effect of ionic strength on coating robustness

The effect of ionic strength on 12mer peptoid microsphere coating robustness was visually assessed by SEM following incubation in various ionic strength solutions (0-500 mM) at pH 6.7 (Figure 9). SEM images demonstrate there is no considerable effect on microsphere morphology at ionic strengths greater than 150 mM (Figure 9A-C). For ionic strength less than 150 mM, microsphere morphology and coverage showed signs of degradation (Figure 9D-F). Specifically, the microspheres appear to fuse together and detach from the surface at ionic strengths less than 100 mM.

As compared to peptide helices, peptoid helices are much more stable when under harsh conditions. As a result, helical peptoids have been demonstrated to be less susceptible to degradation when exposed to various solvent environments (e.g., 2,2,2-trifluorethanol, methanol, and concentrated urea) and high temperatures.[18] However, increasing the ionic strength of the solvent has been demonstrated to stabilize secondary structure for a variety of ionic polypeptides due to screening the electrostatic repulsion between side chains.[55–57] Strongly charged helical peptides are completely destabilized in low ionic strength environments.[58] A similar dependence has been observed in high-ionic strength solutions for peptoids.[18,51] It is hypothesized that the screening of charge-charge repulsive interactions at higher ionic strengths preserves the helical secondary structure that is crucial for microsphere formation. The Hofmeister series claims that

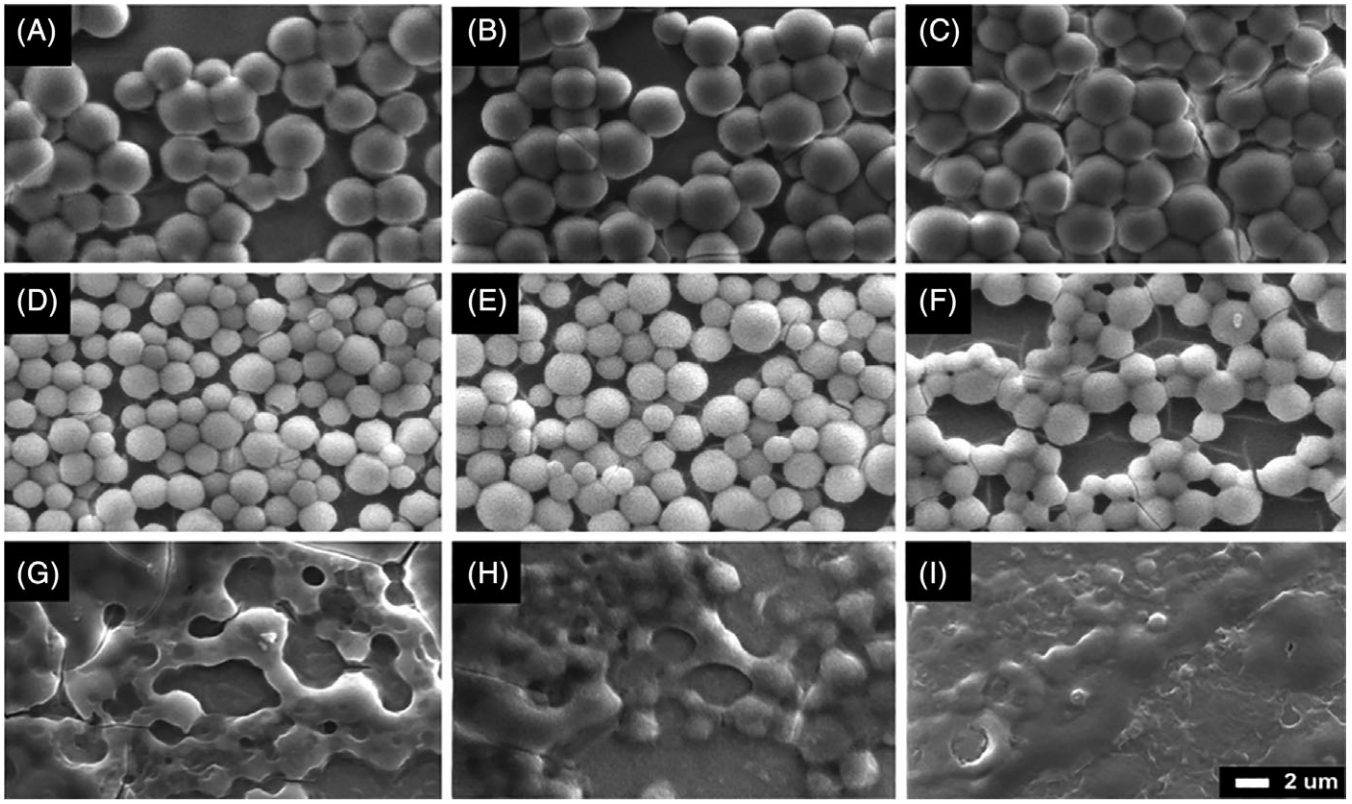

FIGURE 8 SEM images of 12mer peptoid microsphere morphology after 30 minutes in PBS with pH values of (A) 11, (B) 10, (C) 9, (D) 8, (E) 7, (F) 6, (G) 5, (H) 4, or (I) 3

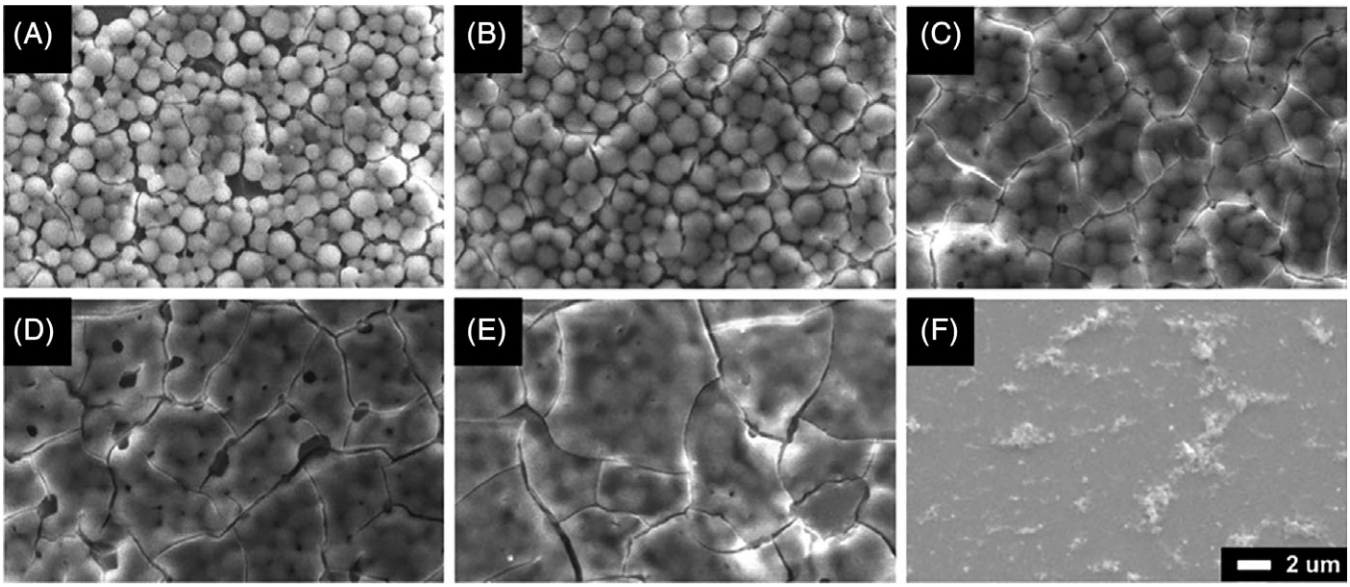

FIGURE 9 SEM images demonstrating the effect of ionic strength on sphere morphology after 30 minutes incubation in water solutions with ionic strengths of (A) 500 mM, (B) 250 mM, (C) 150 mM, (D) 100 mM, (E) 50 mM, and (F) 0 mM

based on the presence of specific ionic compounds there can be a salting "in" or "out" effect that changes the hydrophobicity of the solvent composition, ultimately changing the macromolecules' optical activity and secondary structure.[59–61]

4 | CONCLUSION

In this study, we have shown for the first time that peptoid relative helicity affects the size of microspheres formed, the relative charge location on the microspheres, as well as evaluated the effects of temperature, pH, and ionic strength on the robustness of microsphere coatings. Peptoid microsphere size can be tuned by varying relative helicity, or peptoid chain length (increased length leads to increased helicity). Increased relative helicity leads to smaller peptoid microspheres due to the tight helical secondary structures. Conversely, peptoids with looser helical structures form larger microspheres. The chain length, related to size, also effects the surface charge, as increased chain length had a higher surface zeta potential than the shorter chains. The phase transition temperature for the microsphere coatings increased as the peptoid chain length increased, pointing toward a stability conundrum between helicity and degradative resistance. Future studies will be performed to determine the overall number of peptoid molecules per microsphere, or packing density, using Small Angle X-ray Scattering and Small Angle Neutron Scattering. These current studies have proven that the peptoid microsphere coatings are robust at physiological conditions, as well as high pH and ionic strength solutions. However, under acidic conditions or at low ionic strengths the coatings deteriorate. The ability to tune peptoid microsphere size, as well as stability at physiological conditions, make peptoid coatings promising for use in biosensors and other biomedical applications.

ACKNOWLEDGMENTS

We would like to thank Dr. Rohana Liyanage and the Arkansas Statewide Mass Spectrometry Facility for use of and consultation regarding MALDI, Dr. Mourad Benamara and the University of Arkansas Electron Optics Facility for use of and consultation regarding SEM, Dr. Suresh Kumar for use of and consultation regarding CD, Shu-Ting Chen in Dr. Ranil Wickramasinghe's lab for use of and consultation of zeta potential, and Joshua Tompkins in Dr. David Huitink's lab for use of and consultation regarding DSC. Support has been provided in part by the Arkansas Biosciences Institute, the major research component of the Arkansas Tobacco Settlement Proceeds Act of 2000. Partial support was provided from the Center for Advanced Surface Engineering, under the National Science Foundation Grant No. IIA-1457888 and the Arkansas EPSCoR Program, ASSET III.

ORCID

Shannon L. Servoss https://orcid.org/0000-0003-3075-5423

REFERENCES

[1] T. S. Burkoth, E. Beausoleil, S. Kaur, D. Tang, F. E. Cohen, R. N. Zuckermann, *Chem. Biol.* **2002**, *9*(5), 647.
[2] J. A. Patch, A. E. Barron, *Curr. Opin. Chem. Biol.* **2002**, *6*(6), 872.
[3] R. J. Simon, R. S. Kania, R. N. Zuckermann, V. D. Huebner, D. A. Jewell, S. Banville, S. Ng, L. Wang, S. Rosenberg, C. K. Marlowe, *Proc. Natl. Acad. Sci.* **1992**, *89*(20), 9367.
[4] M. Hagihara, N. J. Anthony, T. J. Stout, J. Clardy, S. L. V. Schreiber, *J. Am. Chem. Soc.* **1992**, *114*(16), 6568.
[5] K. Burgess, H. Shin, D. S. Linthicum, *Angew. Chem. Int. Ed. Engl.* **1995**, *34*(8), 907.
[6] A. B. Smith, D. A. Favor, P. A. Sprengeler, M. C. Guzman, P. J. Carroll, G. T. Furst, R. Hirschmann, *Bioorg. Med. Chem.* **1999**, *7*(1), 9.

[7] D. H. Appella, L. A. Christianson, I. L. Karle, D. R. Powell, S. H. Gellman, *J. Am. Chem. Soc.* **1996**, *118*(51), 13071.
[8] S. Hanessian, X. Luo, R. Schaum, *Tetrahedron Lett.* **1999**, *40*(27), 4925.
[9] C. W. Wu, T. J. Sanborn, R. N. Zuckermann, A. E. Barron, *J. Am. Chem. Soc.* **2001**, *123*(13), 2958.
[10] S. H. Gellman, *Acc. Chem. Res.* **1998**, *31*(4), 173.
[11] J. R. Stringer, J. A. Crapster, I. A. Guzei, H. E. Blackwell, *J. Org. Chem.* **2010**, *75*, 6068.
[12] S. B. Shin, B. Yoo, L. J. Todaro, K. Kirshenbaum, *J. Am. Chem. Soc.* **2007**, *129*, 3218.
[13] K. Huang, C. W. Wu, T. J. Sanborn, J. A. Patch, K. Kirshenbaum, R. N. Zuckermann, A. E. Barron, I. Radhakrishnan, *J. Am. Chem. Soc.* **2006**, *128*, 1733.
[14] P. Armand, K. Kirshenbaum, A. Falicov, R. L. Dunbrack Jr., K. A. Dill, R. N. Zuckermann, F. E. Cohen, *Fold. Des.* **1997**, *2*, 369.
[15] K. Kirshenbaum, A. E. Barron, R. A. Goldsmith, P. Armand, E. K. Bradley, K. T. V. Truong, K. A. Dill, F. E. Cohen, R. N. Zuckermann, *Proc. Natl. Acad. Sci.* **1998**, *95*(8), 4303.
[16] P. Armand, K. Kirshenbaum, R. A. Goldsmith, S. Farr-Jones, A. E. Barron, K. T. V. Truong, K. A. Dill, D. F. Mierke, F. E. Cohen, R. N. Zuckermann, E. K. Bradley, *Proc. Natl. Acad. Sci.* **1998**, *95*(8), 4309.
[17] C. W. Wu, T. J. Sanborn, K. Huang, R. N. Zuckermann, A. E. Barron, *J. Am. Chem. Soc.* **2001**, *123*(28), 6778.
[18] T. J. Sanborn, C. W. Wu, R. N. Zuckermann, A. E. Barron, *Biopolymers* **2001**, *63*(1), 12.
[19] H. Murnen, A. Rosales, J. Jaworski, R. Segalman, R. Zuckermann, *J. Am. Chem. Soc.* **2010**, *132*, 16112.
[20] J. Nam, J. Johnson, J. A. S. Lannutti, *Acta Biomater.* **2001**, *7*, 1516.
[21] X. Chen, K. Ding, N. Ayres, *Polym. Chem.* **2011**, *2*, 2635.
[22] B. Sanii, R. Kudirka, A. Cho, N. Venkateswaran, G. K. Olivier, A. M. Olson, H. Tran, R. M. Harada, L. Tan, R. N. Zuckermann, *J. Am. Chem. Soc.* **2011**, *133*(51), 20808.
[23] E. Robertson, A. P. C. Battigelli, R. Mannige, T. Haxton, L. Yun, S. Whitelam, R. Zuckermann, *Acc. Chem. Res.* **2016**, *49*(3), 379.
[24] M. L. Hebert, D. S. Shah, P. Blake, J. P. Turner, S. L. Servoss, *Org. Biomol. Chem.* **2013**, *11*(27), 4459.
[25] R. N. Zuckermann, J. M. Kerr, S. B. H. Kent, W. H. Moos, *J. Am. Chem. Soc.* **1992**, *114*(26), 10646.
[26] K. T. Nam, S. A. Shelby, P. H. Choi, A. B. Marciel, R. Chen, L. Tan, T. K. Chu, R. A. Mesch, B.-C. Lee, M. D. Connolly, C. Kisielowski, R. N. Zuckermann, *Nat. Mater.* **2010**, *9*(5), 454.
[27] M. L. Waters, *Curr. Opin. Chem. Biol.* **2002**, *6*(6), 736.
[28] A. S. Shetty, J. Zhang, J. S. Moore, *J. Am. Chem. Soc.* **1996**, *118*(5), 1019.
[29] C. G. Claessens, J. F. Stoddart, *J. Phys. Org. Chem.* **1997**, *10*(5), 254.
[30] M. Hebert, D. Shah, P. Blake, S. Servoss, *Coatings* **2013**, *3*(2), 98.
[31] N. Mahmoudi, L. Reed, A. Moix, N. Alshammari, J. Hestekin, S. L. Servoss, *Colloids Surf. B: Biointerfaces* **2017**, *149*, 23.
[32] J. A. Patch, K. Kirshenbaum, S. L. Seurynck, R. N. Zuckermann, A. E. Barron, Versatile oligo(N-substituted) glycines: The many roles of peptoids in drug discovery, in *Pseudo-peptides in Drug Development* (Ed: P. E. Nielsen), Wiley-VCH, Weinheim, Germany **2004**, 1.
[33] I. Gokce, R. W. Woody, G. Anderluh, J. H. Lakey, *J. Am. Chem. Soc.* **2005**, *127*(27), 9700.
[34] Y. Wei, A. Thyparambil, R. Latour, *Biochim. Biophys. Acta* **2014**, *1844* (12), 2331.
[35] S. Mukherjee, G. Zhou, C. Michel, V. A. Voelz, *J. Phys. Chem.* **2015**, *119*(50), 15407.
[36] L. J. Weiser, E. E. Santiso, *AIMS Mater. Sci.* **2017**, *4*(5), 1029.
[37] M. R. Dreher, A. J. Simnick, K. Fischer, R. J. Smith, A. Patel, M. Schmidt, A. Chilkoti, *J. Am. Chem. Soc.* **2008**, *130*(2), 687.
[38] T. Shimada, S. Lee, F. S. Bates, A. Hotta, M. Tirrell, *J. Phys. Chem.* **2009**, *113*(42), 13711.
[39] K. Kornmueller, B. Lehofer, G. Leitinger, H. Amenitsch, R. Prassl, *Nano Res.* **2018**, *11*(2), 913.
[40] S. Gudlur, P. Sukhankar, J. Gao, L. A. Avila, Y. Hiromasa, J. Che, T. Iwamoto, J. M. Tomish, *PLoS ONE* **2012**, *7*(9), e45374.
[41] S. Vauthey, S. Santoso, H. Gong, N. Watson, S. Zhang, *Proc. Natl. Acad. Sci. U. S. A.* **2002**, *99*(8), 5355.
[42] J. D. Hartgerink, E. Beniash, S. I. Stupp, *Science* **2001**, *294*(5547), 1684.
[43] J. D. Hartgerink, J. R. Granja, R. A. Milligan, M. R. Ghadiri, *J. Am. Chem. Soc.* **1996**, *118*(1), 43.
[44] L. Adier-Abramovich, P. Marco, Z. A. Arnon, R. C. Creasey, T. C. Michaels, A. Levin, D. J. Scurr, C. J. Roberts, T. P. Knowles, S. J. Tendler, E. Gazit, *ACS Nano* **2016**, *10*(8), 7436.
[45] Y.-H. Chiao, A. Sengupta, S.-T. Chen, S.-H. Huang, C.-C. Hu, W.-S. Hung, Y. Chang, X. Qian, S. Wickramasinghe, K.-R. Lee, J.-Y. Lai, *Sep. Purif. Technol.* **2019**, *212*, 316.
[46] M. H. Chiu, E. J. Prenner, *J. Pharm. Bioallied Sci.* **2011**, *3*(1), 39.
[47] D. Giron, *J. Therm. Anal. Calorim.* **2002**, *68*(2), 335.
[48] B. Sauer, W. Kampert, E. N. Blanchard, S. Threefoot, B. Hsiao, *Polymer* **2000**, *41*(3), 1099.
[49] V. Maravajhala, N. Dasari, A. Sepuri, S. Joginapalli, *Indian J. Pharm. Sci.* **2009**, *71*(6), 663.
[50] L. Malavolta, M. R. Pinto, J. H. Cuvero, C. R. Nakaie, *Protein Sci.* **2006**, *15*(6), 1476.
[51] S. Shin, K. Kirshenbaum, *Org. Lett.* **2007**, *9*(24), 5003.
[52] J. Kim, J. Mao, M. Gunner, *J. Mol. Biol.* **2005**, *348*, 1283.
[53] D. Bashford, *Front. Biosci.* **2004**, *9*, 1082.
[54] J. Dwyer, A. Gittis, D. Karp, E. Lattman, D. Spencer, W. E. Stites, B. Garcia-Moreno, *Biophys. J.* **2000**, *79*(3), 1610.
[55] M. van der Graaf, M. Hemminga, *FEBS J.* **1991**, *201*(2), 489.
[56] W. Kohn, C. Kay, R. Hodges, *Protein Sci.* **1995**, *4*, 237.
[57] I. Jelesarov, E. Durr, R. Thoma, H. Bosshard, *Biochemistry* **1998**, *37*, 7539.
[58] M. Hoshino, N. Yumoto, S. Yoshikawa, Y. Goto, *Protein Sci.* **1997**, *6* (7), 1396.
[59] H. I. Okur, J. Hladilkova, K. B. Rembert, Y. Cho, J. Heyda, J. Dzubiella, P. S. Cremer, P. Jungwirth, *J. Phys. Chem.* **2017**, *121*(9), 1997.
[60] A. H. Crevenna, N. Naredi-Rainer, D. C. Lamb, R. Wedlich-soldner, J. Dzubiella, *Biophys. J.* **2012**, *102*(4), 907.
[61] Y. Zhang, P. S. Cremer, *Curr. Opin. Chem. Biol.* **2006**, *10*(6), 658.

SUPPORTING INFORMATION

Additional supporting information may be found online in the Supporting Information section at the end of this article.

How to cite this article: Perez Bakovic GR, Roberts JL, Colford B, Joyce M, Servoss SL. Peptoid microsphere coatings: The effects of helicity, temperature, pH, and ionic strength. *Biopolymers*. 2019;e23283. https://doi.org/10.1002/bip.23283